Investigation of wind turbine gearbox bearing subsurface damage considering transient loading

H. Al-Tameemi[1], H. Long[2] and R.S. Dwyer-Joyce
Department of Mechanical Engineering, The University of Sheffield, United Kingdom
[1]Presenting author
[2]Corresponding author: h.long@sheffield.ac.uk
Tel: +44 (0) 114 222 7759
Fax: +44 (0) 114 222 7890

Abstract

In this study, a failed bearing in planetary gear stage of a sub megawatt wind turbine gearbox is destructively investigated to identify different stages and features of the premature damages induced. The focus is on the role of Manganese Sulphide (MnS) inclusion in subsurface initiated damage of White Etching Areas (WEAs) and White Etching Cracks (WECs). The main types are grouped as (1) undamaged MnS inclusions; (2) inclusions separated from the matrix by gaps; (3) internal micro cracks of the inclusions; (4) micro cracks initiated from inclusions into the steel matrix; and (5) WEA around the inclusion (Butterflies). Alongside this work, the load, maximum contact pressure and subsurface stresses are calculated for the planetary bearing of NREL (National Renewable Energy Laboratory) 750 kW wind turbine during three operational conditions: shutdown, start up and normal operation. The high subsurface stress levels due to transient loading and the stress concentration around the MnS inclusion are correlated to the yielding of the material. The depth of the maximum shear stress is correlated to the dominated depth of the subsurface micro cracks. This study highlights the role of the separation of the MnS inclusions and surface traction in the subsurface initiated damage of wind turbine gearbox bearings.

Keywords

WEA/ WECs/ butterflies, wind turbine bearings, subsurface damage, non-metallic inclusions.

1. Introduction

The reliability of wind turbine plays a significate role in reducing wind energy costs. Maintenance and downtime need to be reduced to the minimum. This could be achieved by improving the endurance of the most often replaced parts. Although the failure rate of bearings in wind turbine application is less than other components, the costs for their replacement and maintenance and the downtime caused by their failure put their reliability as a priority among other components [1]–[4]. Therefore, bearings still require further investigation to reach a satisfactory operation life.

Premature bearing failures have been frequently observed in wind turbine gearboxes. The failures may initiate either on the surface or near the surface of contact in the bearing raceways [5]–[7]. The surface initiation hypothesis suggests that cracks could be caused by surface flaws and worsen by loading conditions [6], [8], [9]. On the other hand, manufacturing factors such as the non-metallic inclusions could serve as damage initiators, according to the sub-surface hypothesis [10]–[12]. The various hypotheses have been proposed including the effect of hydrogen, plastic deformation, brittle fracture due to high traction on the surface, and unconsidered loadings, such as impact load, causing lubrication failure [13]–[16]. However, a clear explanation with sufficient evidence based on both the effecting factors such as the high loading during the transient operation events and the observed premature damages such as the White Etching Cracks (WEC) is not established.

In this study, a destructive investigation of a failed sub megawatt wind turbine planetary bearing is carried out. The aim is to investigate the effect of Manganese Sulphides (MnS) inclusions on the initiation of subsurface damage. The characteristics of the damaged inclusions and micro cracks are analysed and correlated to the subsurface stresses. To investigate the effect of surface traction, the load on the planetary bearings is calculated at different operation conditions and linked to the observed depth of subsurface damage.

2. White Etching Cracks and Rolling Contact Fatigue

Before studying the premature failure of White Structure Flacking (WSF), the final stage of White Etching Cracks (WECs), it is necessary to consider damages resulted from classical Rolling Contact Fatigue (RCF) failure. Therefore, the damage features, loading conditions and occurrence time for each of the damages are outlined in this section. The White Etching Area (WEA) represents microstructure changes in high strength steel when observed under the microscopic examination. This can be observed after the sample is polished and etched with nital (~ 2% nitric acid in ethanol) or picral [6], [17], [18]. Comparing to the RCF induced WEAs, the microstructure changes shown in the premature WSF, are not uniform in shape or distribution, that is why it is also called the irregular White Etching Area (irWEA) [16], [19]. While in the RCF, it shows a structure of 30º or 80º inclined angle to the rolling direction and it is usually called flat or steep White Bands (WBs). In addition, their density of occurrence is much less than that in the RCF [16], [18], [20]–[22]. Many studies were conducted to investigate the onset values of contact pressure P and number of cycles Nc required to start WEAs in the RCF. It has been proven that the microstructure changes to cause WBs starts at P> 2.5 GPa and Nc >10^7 cycles [22], [23]. On the other hand, the premature failure by WSF could happen at moderate number of cycles [23].

3. Destructive investigation of a failed bearing

The investigated bearing was used in a planetary stage of a sub megawatt wind turbine. The visual observation showed extreme surface damage in the inner race comparing to the outer race. The inner race is destructively investigated by preparing samples for microscopic examination. The first step in sample preparation is to section the inner race to smaller parts where the subsurface of radial and axial sections can be examined. Figure 1 shows the sectioning pattern adopted. A variety of sections from different locations of the bearing has been created such as the severely damaged surface, the lightly damaged surface and the visually non damaged surface. After the grinding and polishing up to the mirror like surface, the samples have been etched with nital. The microscopic examination of the subsurface area covered more than 1 mm depth from the surface. Because the structure of the WEA differs from the non-altered area, these WEA will appear in a lighter colour under optical microscopy. Etching is important to reveal the microstructure alternation such as WEA and WECs but it is not recommended to reveal other features such as the separation of the inclusion from the steel matrix. Although most of the images analysed have been acquired by using optical microscopy, images of more detailed microstructure features have been acquired using Scanning Electron Microscopy (SEM) which reveal the size and the topography of the WEA as well as the size and the directions of the micro cracks inside the inclusion and the matrix. Further characterization of the separation of the inclusions from the matrix and the chemical elements of the inclusions is curried out using the Energy Dispersive Spectroscopy (EDS). Also, the Atomic Force Microscopy (AFM) is utilized to show clearly the gaps or separation attached to the MnS inclusion, as well as the micro cracks.

4. Load and stress on surface and subsurface of planetary bearing

In this study, a simplified calculation procedure is proposed to calculate the load on the planetary bearing of the NREL 750 kW wind turbine. This calculation method is validated against the Gearbox Reliability Collaborative (GRC) project [24]. An exact comparison is not possible because the numerical values of loads are not provided in the report of NREL. However, the estimated average values are used in the comparison as shown in Table 1. The simplicity of the proposed calculation method and the relatively small percentage error show a good compromise between calculation complexity and accuracy.

Table 1: Comparison for the average planet–sun gear contact load levels

	Loads (kN)		
	Circumferential	Radial	Axial
This study	180.56	66.284	23.771
Average of GRC results	175	70	23
Approximate percentage error	3.1771	5.3086	3.3522

The torque and speed measured at the low speed shaft are used to calculate the radial load acting on each planetary bearing as shown in Equation 1.

$$F_r = \frac{Torque_{in} * \omega_c}{3 * R_s * \omega_s} \quad (1)$$

The radial load on the upwind bearing is calculated assuming 50% more than that on the downwind bearing [25]. The maximum contact pressure on the inner race is calculated based on the Hertzian contact theory, Equation 2. In this equation Q_0 is the maximum roller-raceway normal load, b is the half width of contact and L is the contact length. Equations 3 and 4 are the subsurface stress components calculated from the maximum contact pressure. The maximum subsurface shear stress τ_1 is calculated from Equation 5 with $\tau_{xz} = 0$ at the middle of the contact [26].

$$p_{max} = \frac{2 * Q_0}{\pi * L * b} \quad (2)$$

$$\sigma_{xx} = -p_{max}\left\{\left(\frac{1 + 2\frac{z^2}{b^2}}{\sqrt{1 + \frac{z^2}{b^2}}}\right) - 2 * \left|\frac{z}{b}\right|\right\} \quad (3)$$

$$\sigma_{zz} = \frac{-p_{max}}{\sqrt{1 + \frac{z^2}{b^2}}} \quad (4)$$

$$\tau_1 = \sqrt{\left(\frac{\sigma_{xx} - \sigma_{zz}}{2}\right)^2 + \tau_{xz}^2} \quad (5)$$

Figure 1: Main sections and subsections of the failed bearing

5. Observed MnS inclusions

The light grey inclusions found in this bearing steel is classified according to the British standard E45 as Type A-Sulphide which could be manganese sulphides or aluminates embedded in manganese sulphide [27]. Determining the exact components of these inclusions was performed using energy dispersive x-ray analysis and showed Manganese (Mn) and Sulphur (S). No Aluminium (Al) is found at the dark tips of the inclusions which are found to be gaps/separations using AFM and SEM. In radial sections, the general features of the observed inclusions are an elliptical shape of different length and width with pointed ends, inclined at different angle to the surface, and at different depth from the surface. Comparing to the radial sections, the difference observed in the axial sections is that the inclusions have less uniform shapes and in most cases, they are ellipses of less inclination.

6. Subsurface damages and statistics

The observed damages vary between surface and subsurface as shown in Figure 2 (a). The failures may initiate either on the surface or near the surface of contact in the bearing raceways. In this study, the examination is focused on the subsurface initiated damage at the MnS inclusions and the surrounding steel matrix which are marked in Figure 2 (b) and (c). The observations are classified into five types which are undamaged inclusions, inclusions separate from the matrix by gap(s), internal cracks of the inclusions, cracks initiate from inclusions into the steel matrix, WEA around the inclusion (Butterflies). Statistical study associated with each specified damage type is carried out. Figure 3 shows the percentage of each of the observed damage types out of more than 200 MnS inclusions. Figure 4 (a) and (b) show some of the characteristics of the micro cracks associated with MnS inclusions. It can be seen that the dominant crack angle in the axially sectioned samples is almost zero and in circumferentially sectioned samples is closer to the inclusion angle. Also, cracks in circumferentially sectioned samples are more proportional to the inclusion size than cracks in the axially sectioned samples. The investigation on the MnS inclusion in the literature is less reported than the harder inclusions such as Al_2O_3 because it is assumed that the MnS inclusion always deforms without causing gaps attached to it. However, in this study, the results of the AFM, Figure 2 (c), shows that this is not always the case. Because the MnS inclusion separation from the matrix occurred at different depths to the contact surface, sometimes far from the loaded zone, it could be considered that the material defect is caused by the different coefficient of thermal expansion [20]. However, other types of separation could be caused by impact loading [28]. The non-perfect bonding and separation of the MnS inclusions result in high stress concentration around the inclusions [29]. WEA is a microstructure alternation which is expected to occur at the location of high stress concentration, eventually causing the material yielding. This explains their irregular shapes which differ from the flat or steep White Bands (WB) occurred due to the RCF. This also explains the association of high percentage of the observed WEA, butterflies, with the separated inclusions. Another interesting observation is the internal cracking of MnS inclusions. It is found that inclusion cracking could be accompanying by other types of subsurface damages.

7. Contact pressure and subsurface stress under different operation conditions

In this study, the 750 kW NREL wind turbine is used to calculate the load and stresses induced on the bearing. The maximum contact pressure on the inner raceway of the planetary bearing during different operational conditions can be seen in Figure 5. These results show that the maximum contact pressure exceeds the maximum contact pressure recommended in the design standards [30] and [31]. However, this contact pressure will not cause a subsurface yielding of the through hardened bearing steel if the effect of inclusions and gaps is neglected. It is generally assumed that bearings working under lubricated condition are exposed to low traction force. Nevertheless, during the transient events a very low lubricant film thickness, relative to the bearing surface roughness, could occur that elevates the traction force. This surface traction results in additional subsurface stress and brings the location of the maximum shear stress closer to the surface. It has been found that the maximum shear stress, from the calculations of the subsurface stresses, is located deeper than the dominated depth of the micro cracks, from the failed bearing examination as shown in Figure 6. This shows the significant effect of the surface traction on the subsurface initiated damage.

a

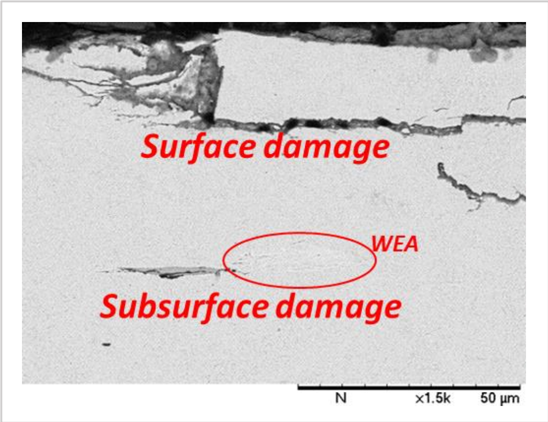

b

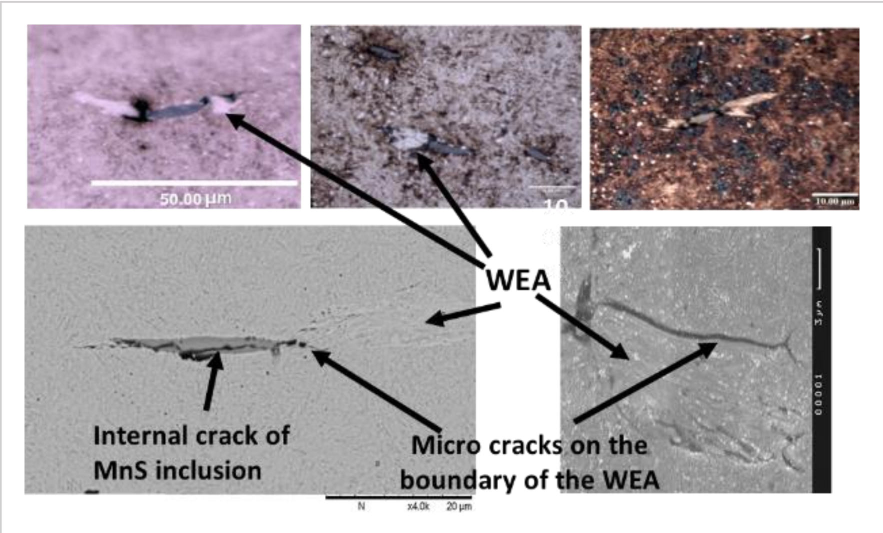

c

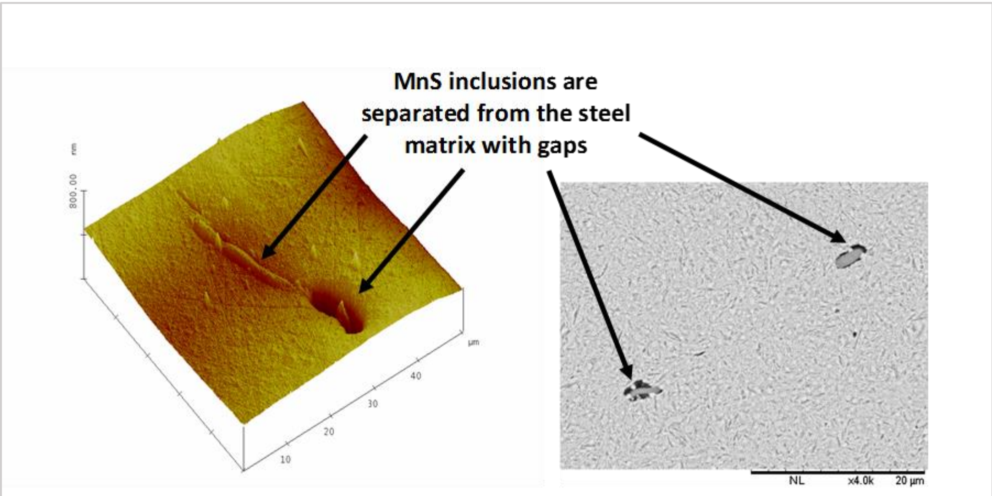

Figure2: Surface and subsurface damages in the failed wind turbine bearing

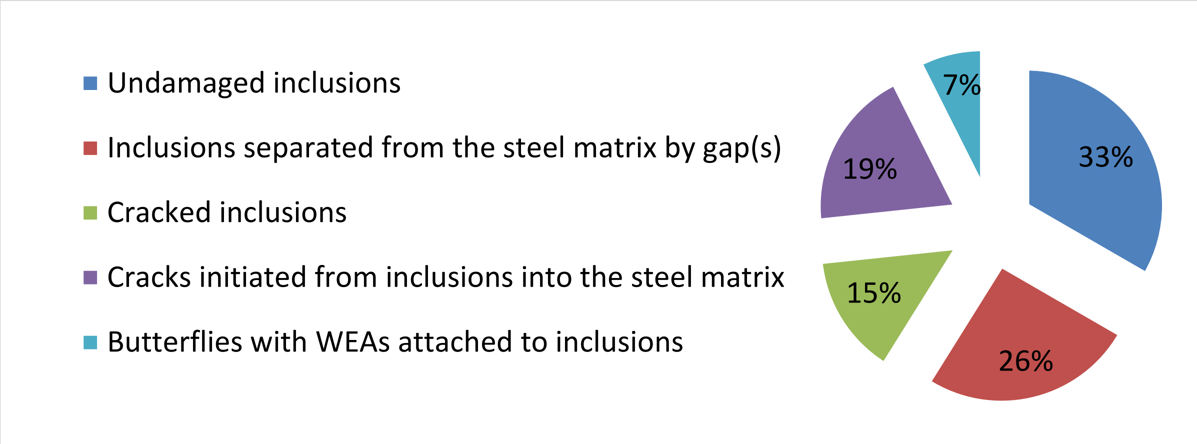

Figure3: Observed subsurface damage types at MnS inclusions

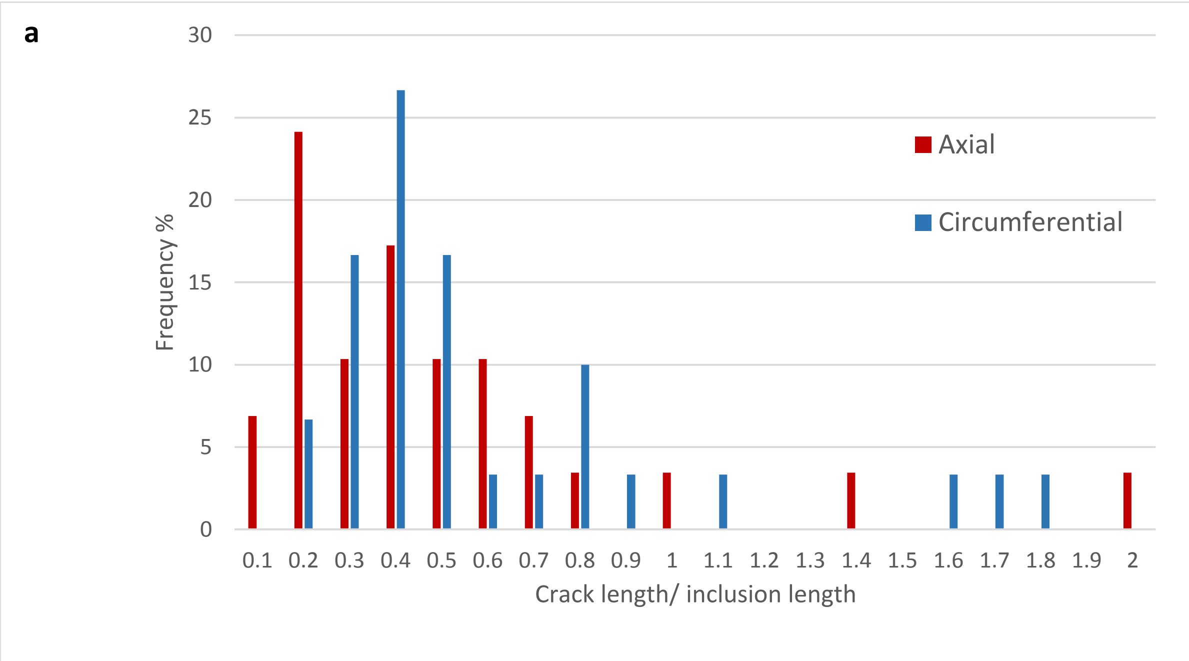

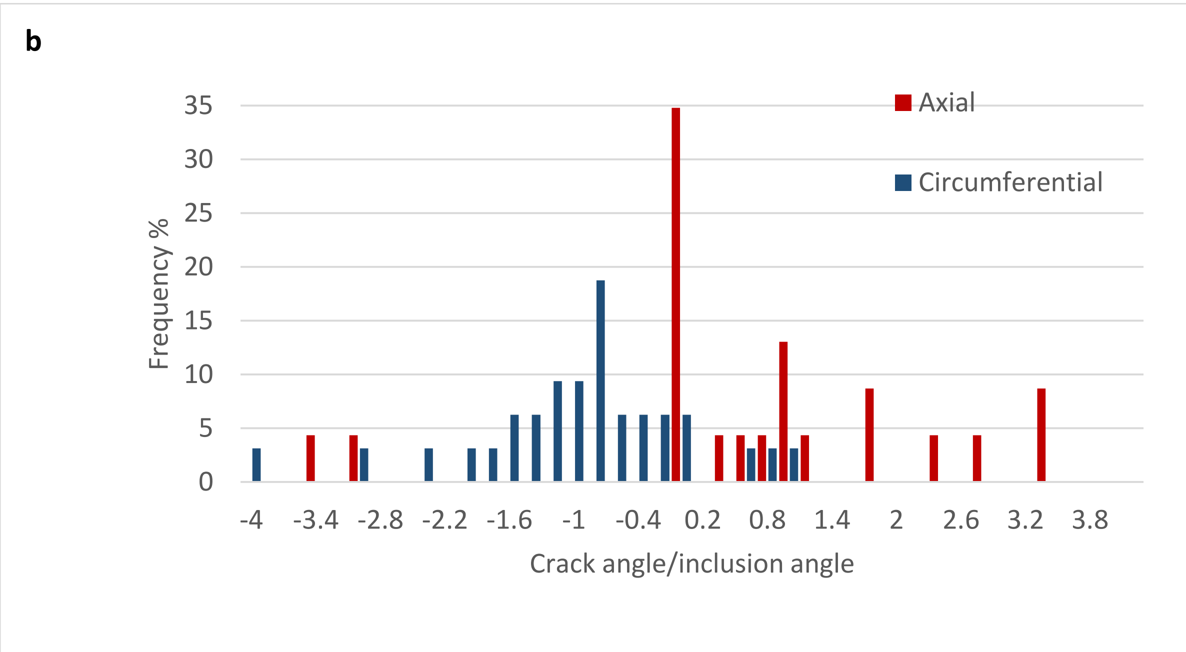

Figure 4: Damage characteristics (a) relative micro cracks length (b) relative micro cracks angle

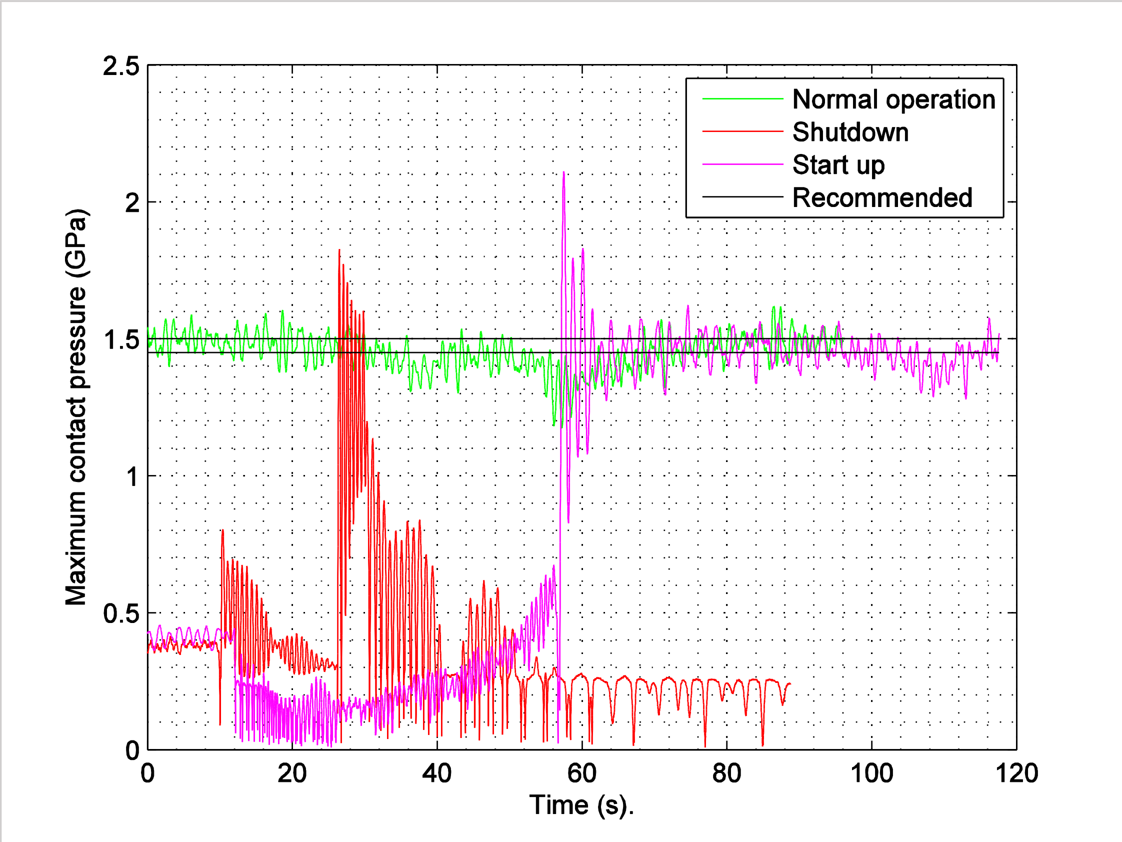

Figure 5: Maximum contact pressure at the inner ring of planetary bearing

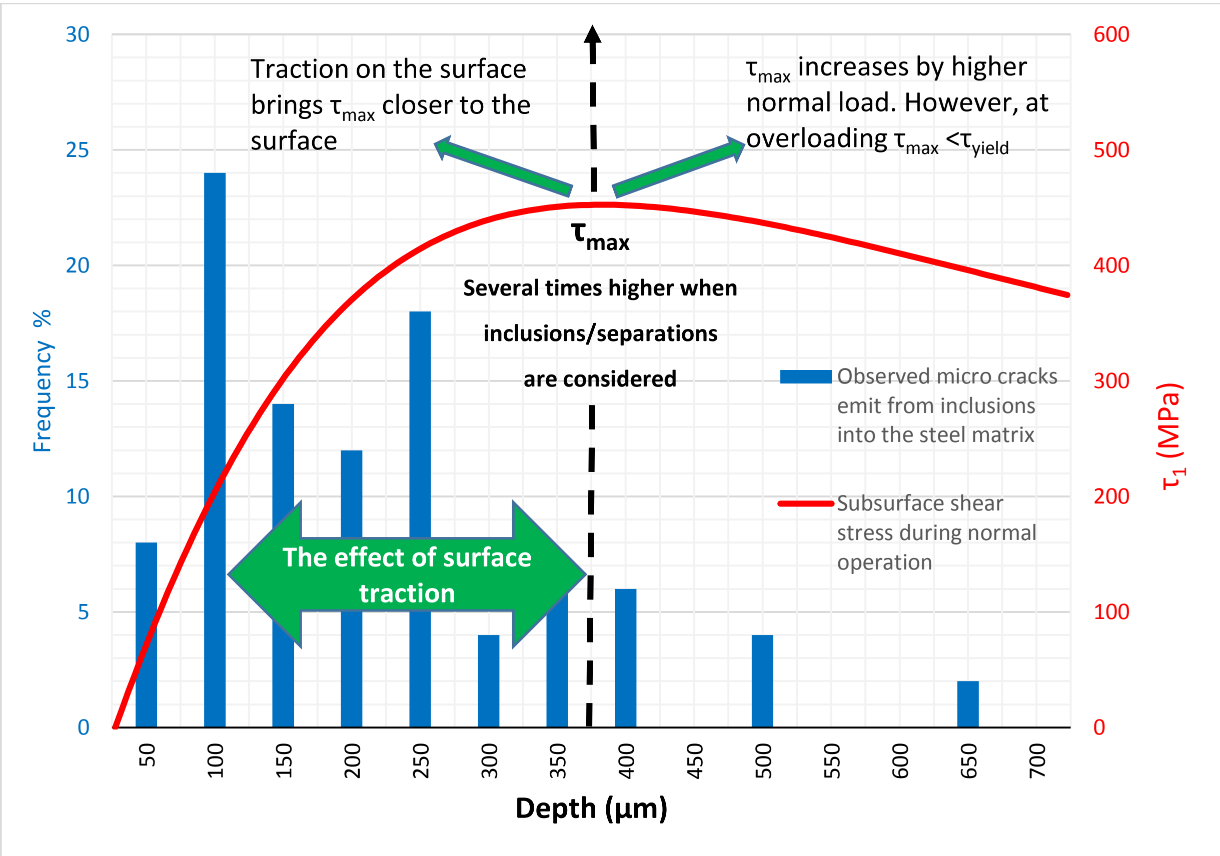

Figure 6: Depth of micro cracks comparing with depth of subsurface maximum shear stress

8. Conclusions

The distractive investigation of a wind turbine bearing failed prematurely provided insight to the subsurface initiated damage at the MnS inclusion. In addition to the surface damage of pitting, spalling and wide and shallow cracks initiated on the surface, four types of subsurface damage are observed which are expected to be the reason for the bigger spalls and the faster deterioration of the bearing life. These are inclusions separated from the matrix by gaps; internal micro cracks of the inclusions; micro cracks initiate from inclusions into the steel matrix; WEA around the inclusion (Butterflies). The analysis of these observations helps drawing up the following conclusions.

1. It is found that the separation of MnS inclusions from the matrix occurs at different levels of depth to the contact surface, sometimes far from the load zone. Accordingly, it is possible that this defect is caused by the different coefficient of thermal expansion during manufacturing although it is believed that other kind of separation could be caused by loading.
2. If the non-perfect bonding, separation, of the MnS inclusion is considered in stress calculation around the inclusions, local yielding may occur which matches the observed WEA around the separation and inclusions.
3. Load and contact pressure calculation showed higher level than the recommended values. However, the subsurface maximum shear stress at the highest load during transient events is still less than the yielding value. This highlights the effect of gaps, separation, in concentrating and increasing the stress to the critical damaging level in the form of WEA or micro cracks.
4. Correlating the depth of the subsurface damage of micro cracks on the MnS inclusions to the depth of the maximum shear stress revealed the occurrence of considerable surface traction. The surface traction brings the location of the maximum shear stress, potentially subsurface damage location, closer to the contact surface.

Acknowledgement

The first author would like to thank the Iraqi Ministry of Higher Education and Scientific Research http://www.igmohe.gov.iq for funding his study. Also, the authors would like to thank the anonymous industrial partner for the provision of the failed bearing.

References

[1] S. Faulstich, B. Hahn, H. Jung, and K. Rafik, "Suitable failure statistics as a key for improving availability," *Proc. Eur. Wind Energy Conf. EWEC*, p. Online resource, 2009.

[2] S. Faulstich and B. Hahn, "Comparison of different wind turbine concepts due to their effects on reliability," *Contract*, pp. 1–20, 2009.

[3] J. Ribrant and L. M. Bertling, "Survey of failures in wind power systems with focus on Swedish wind power plants during 1997-2005," *IEEE Trans. Energy Convers.*, vol. 22, no. 1, pp. 167–173, 2007.

[4] S. K. G, I. D, B. N, C. J, and S. A, "Effects of Extreme and Transient Loads on Wind Turbine Drive Trains," *Proc. 30th ASME Wind Energy Symp.*, pp. 1–24, 2012.

[5] R. Wood, J. Basumatary, and M. Evans, "Energy-related tribo-corrosion research at the National Centre for Advanced Tribology at Southampton," *ASTM STP*, pp. 169–202, 2013.

[6] S. K. F. Gmbh, GE Drivetrain Technologies, and H. C. Rogers, "Premature bearing failures in industrial gearboxes Lagerfrühausfälle in Industriegetrieben Kenred Stadler ° Arno Stubenrauch *," *Annu. Rev. Mater. Sci.*, vol. 9, no. 1, pp. 283–311, 2013.

[7] R. Errichello, R. Budny, R. Eckert GEARTECH, R. Eckert, and G. Townsend, "Investigations of Bearing Failures Associated with White Etching Areas (WEAs) in Wind Turbine Gearboxes," *Tribol. Trans.*, vol. 566, no. 56, pp. 1069–1076, 2013.

[8] B. Gould and A. Greco, "The Influence of Sliding and Contact Severity on the Generation of White Etching Cracks," *Tribol. Lett.*, vol. 60, no. 2, 2015.

[9] B. Gould and A. Greco, "Investigating the Process of White Etching Crack Initiation in Bearing Steel," *Tribol. Lett.*, vol. 62, no. 2, 2016.

[10] M. Brückner, J. Gegner, A. Grabulov, W. Nierlich, and J. Slycke, "Butterfly formation mechanisms in rolling contact fatigue," *Proc VHCF-5*, pp. 101–106.

[11] J.-H. Kang, R. H. Vegter, and P. E. J. Rivera-Díaz-del-Castillo, "Rolling contact fatigue in martensitic 100Cr6: Subsurface hardening and crack formation," *Mater. Sci. Eng. A*, vol. 607, pp. 328–333, 2014.

[12] A. Warhadpande, F. Sadeghi, M. N. Kotzalas, and G. Doll, "Effects of plasticity on subsurface initiated spalling in rolling contact fatigue," *Int. J. Fatigue*, vol. 36, no. 1, pp. 80–95, 2012.

[13] A. Greco, "Bearing Reliability- White Etching Cracks (WEC)," in *Gearbox Reliability Collaborative Annual Meeting*, 2014.

[14] H. Uyama, "The mechanism of white structure flaking in rolling bearings," *Natl. Renew. energy Lab. Wind turbine*, pp. 1–37, 2011.

[15] H. Uyama, H. Yamada, H. Hidaka, and N. Mitamura, "The Effects of Hydrogen on Microstructural Change and Surface Originated Flaking in Rolling Contact Fatigue," *Tribol. Online*, vol. 6, no. 2, pp. 123–132, 2011.

[16] R. Errichello, S. Sheng, J. Keller, and A. Greco, "Wind Turbine Tribology Seminar," pp. 15–17, 2011.

[17] M.-H. Evans, "White structure flaking (WSF) in wind turbine gearbox bearings: effects of 'butterflies' and white etching cracks (WECs)," *Mater. Sci. Technol.*, vol. 28, no. 1, pp. 3–22, 2012.

[18] a. Ruellan, F. Ville, X. Kleber, a. Arnaudon, and D. Girodin, “Understanding white etching cracks in rolling element bearings: The effect of hydrogen charging on the formation mechanisms,” *Proc. Inst. Mech. Eng. Part J J. Eng. Tribol.*, vol. 228, no. 11, pp. 1252–1265, 2014.
[19] M. H. Evans, A. D. Richardson, L. Wang, and R. J. K. Wood, “Serial sectioning investigation of butterfly and white etching crack (WEC) formation in wind turbine gearbox bearings,” *Wear*, vol. 302, no. 1–2, pp. 1573–1582, 2013.
[20] H. K. D. H. Bhadeshia, “Steels for bearings,” *Prog. Mater. Sci.*, vol. 57, no. 2, pp. 268–435, 2012.
[21] J. Gegner, “Tribological Aspects of Rolling Bearing Failures,” *C.-H. Kuo (ed.), Tribol. Lubr.*, pp. 33–94, 2011.
[22] P. E. J. Rivera-Díaz-del-Castillo, “Rolling contact fatigue in bearings: Phenomenology and modelling techniques,” *ASTM Spec. Tech. Publ.*, vol. 1548 STP, pp. 355–381, 2012.
[23] G. L. Doll, “Tribological Challenges in Wind Turbine Technology,” *NREL Wind turbine Tribol. Semin.*, 2011.
[24] H. Link, W. Lacava, J. Van Dam, and B. Mcniff, “Gearbox Reliability Collaborative Project Report : Findings from Phase 1 and Phase 2 Testing,” no. June, p. 85, 2011.
[25] W. LaCava, J. Keller, and B. McNiff, “Gearbox Reliability Collaborative: Test and Model Investigation of Sun Orbit and Planet Load Share in a Wind Turbine Gearbox; Preprint,” *Nrel*, no. April, 2012.
[26] R. G. Budynas, J. K. Nisbett, and J. E. Shigley, *Mechanical engineering design*. 2011.
[27] ASTM, “E45 Standard Test Methods for Determining the Inclusion Content of Steel,” 1997.
[28] T. Bruce, H. Long, T. Slatter, and R. S. Dwyer-Joyce, “Formation of white etching cracks at manganese sulfide (MnS) inclusions in bearing steel due to hammering impact loading,” *Wind Energy*, 2016.
[29] “METAL FATIGUE: EFFECTS OF SMALL DEFECTS AND NONMETALLIC INCLUSIONS, 1st Edition | Yukitaka Murakami | ISBN 9780080440644.” .
[30] ANSI/AGMA/AWEA 6006-A03, “standard for design and specification of gearbox of wind turbine 6006-a03.pdf.” 2004.
[31] *Wind turbines Part 4: Design requirements for wind turbine gearboxes*. BSI Standards Publication, 2013.